

**MODULAR MACRO INVERTER  
FOR  
“INTELLIGENT POWER CONTROLLERS FOR  
SELF-ORGANIZING MICROGRIDS \***

S.F. Glover, F.E. White, S.V. Spires

February 2, 2009

---

\* Sandia National Laboratories is a multi-program laboratory managed and operated by Sandia Corporation, a wholly owned subsidiary of Lockheed Martin Corporation, for the U.S. Department of Energy's National Nuclear Security Administration under contract DE-AC04-94AL85000.

## TABLE OF CONTENTS

<b>I. INTRODUCTION .....</b>	<b>3</b>
A. Circuit Model .....	3
B. Average Value Model (Continuous operation) .....	4
<b>II. DUTY RATIO.....</b>	<b>6</b>
<b>III. CONTINUOUS VERSUS DISCONTINUOUS OPERATION .....</b>	<b>6</b>
<b>IV. DC LINK VOLTAGE RIPPLE.....</b>	<b>7</b>
<b>V. AMPLITUDE MODULATION RATIO .....</b>	<b>8</b>
<b>VI. OUTPUT FILTER .....</b>	<b>8</b>
<b>VII. OUTPUT TRANSFORMER .....</b>	<b>8</b>
<b>VIII. BOOST CONTROL .....</b>	<b>8</b>
<b>IX. INVERTER CONTROL.....</b>	<b>8</b>
<b>X. THERMAL ANALYSIS.....</b>	<b>8</b>
A. Boost converter with heat sink fan .....	9
B. Boost converter without heat sink fan .....	10
C. Inverter .....	10
<b>XI. COMPONENT BASED POWER DERATING.....</b>	<b>12</b>
<b>XII. CONDUCTION BASED POWER DERATING.....</b>	<b>12</b>
<b>XIII. SENSOR SIGNAL FILTERS.....</b>	<b>12</b>
<b>XIV. INPUTS AND OUTPUTS .....</b>	<b>13</b>
<b>XV. PHOTOGRAPHS OF THE MMI .....</b>	<b>13</b>
<b>XVI. REFERENCES .....</b>	<b>15</b>
<b>XVII. APPENDIX - PARTS LIST .....</b>	<b>16</b>
<b>XVIII. APPENDIX – WIRING DIAGRAM .....</b>	<b>17</b>
<b>XIX. APPENDIX – H-BRIDGE CURRENT SENSOR.....</b>	<b>18</b>

## I. INTRODUCTION

Power electronic based inverters have proven to be a key element to the connection of renewable resources to the grid. Research into the control of these inverters needs to improve load sharing capabilities, islanding capabilities, reliability, and greater understanding of sources that are close in proximity. The inverter design presented in this document has been setup as a research platform for further research into reliable renewable energy resources. The power supply presented below is referred to as a modular macro inverter (MMI). The design requirements for the MMI are listed in Table I below.

Table I. Design Requirements

1	The MMI shall be attachable to a solar panel.
2	The MMI shall supply up 1kW or greater of power.
3	The MMI shall be capable of operating over a DC voltage input range of 12V to 48V
4	The MMI shall be capable of outputting a 60 Hz, 120 Vrms waveform.
5	The MMI shall be controllable to the switching level.
6	The MMI should be designed so that it could self charge from the output side of the power supply.
7	The control design will be performed separate from the hardware design and therefore is not included in this document.
8	An average value circuit model shall be included for control development
9	The MMI should be constructed by the end of FY08 if resources permit.

The actual MMI specifications after completion of the design are listed in Table II. Note that the power and voltage range requirements have been met. This power supply can run off of a DC source solar panels included. Direct control over the IGBTs is also a design feature allowing the future control design to operate down to the switching level.

Table II. Design Specifications

Input voltage range	0 – 250V
Maximum power	1.2 kW
Maximum boost converter switching frequency	10kHz
Maximum inverter switching frequency	10kHz
DC isolated output (minimum)	300V
Maximum DC link voltage	250 V
Maximum input current	25 A
Maximum output current	10 Arms
Output voltage	120 Vrms

The power electronics reference used throughout this design was Mohan [1]. All analysis and simulations presented below were performed using MatLab [2].

### A. Circuit Model

The circuit diagram is provided in Figure 1 and includes blocks representing the controllers. The circuit parameters are listed in Table III and are followed by the differential equations that describe the behavior of the circuit. Heaviside's notation is used in the equations. That is  $px = dx/dt$ .

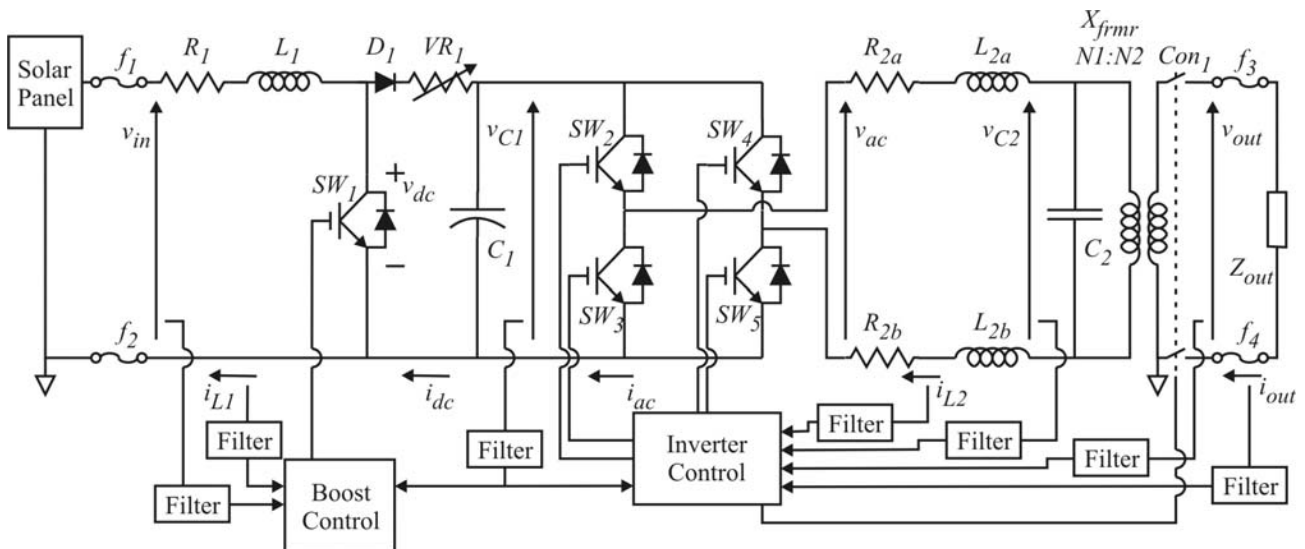


Figure 1. MMI circuit model.

Table III. Circuit Parameter Values

Resistance of $L_1$	$R_1$	<15 mΩ
Resistance of $L_{2a}$	$R_{2a}$	15 mΩ
Resistance of $L_{2b}$	$R_{2b}$	15 mΩ
Thermistor <sup>1</sup>	$VR_1$	18.5 mΩ – 1 Ω 214 °C – 25 °C
Boost inductance <sup>2</sup>	$L_1$	1 mH
Filter inductance <sup>2</sup>	$L_{2a}$	1 mH
Filter inductance <sup>2</sup>	$L_{2b}$	1 mH
DC link capacitance	$C_1$	4.2 mF
Filter capacitance	$C_2$	35 μF
Isolation transformer	$X_{frmr}$	1:1
Input fuse	$f_1, f_2$	35 Adc
Output fuse	$f_3, f_4$	10 Arms

<sup>1</sup> The thermistor is in series with  $D_1$  and  $C_1$  to act as a inrush current limiter, two devices are in parallel.

<sup>2</sup> Note that the inductors were vacuum impregnated with epoxy to reduce the audible noise [3].

The derivative of the current through  $L_1$  is

$$p i_{L1} = \frac{(v_{in} - i_{L1} R_1 - v_{dc})}{L_1}, \quad (1)$$

where  $v_{dc}$  is the voltage across  $SW_1$ . The derivative of the voltage across  $C_1$  is

$$pv_{C1} = \frac{(i_{dc} - i_{ac})}{C_1}, \quad (2)$$

where  $i_{dc}$  is the current flowing through  $D_1$  and  $i_{ac}$  is the current into the inverter. The derivative of the current through  $L_2$  is

Figure 2. MMI average value model.

$$pi_{L2} = \frac{(v_{ac} - i_{L2}R_2 - v_{C2})}{L_2}, \quad (3)$$

where  $v_{ac}$  is the voltage at the output of the inverter,  $L_2$  is the total inductance of the filter

$$L_2 = L_{2a} + L_{2b}, \quad (4)$$

and  $R_2$  is the total resistance of the filter inductor

$$R_2 = R_{2a} + R_{2b} . \quad (5)$$

The derivative of the voltage across  $C_2$  is

$$pv_{C2} = \frac{(i_{L2} - i_{out} N1N2)}{C_2}, \quad (6)$$

where  $N1N2$  is the turns ratio of  $X_{frmr}$ . The voltage at the output side of the contactor,  $Con_1$ , is

$$v_{out} = v_{C2} N1N2 . \quad (7)$$

The current out of the MMI is defined as

$$i_{out} = \frac{v_{out}}{Z_{out}} . \quad (8)$$

### *B. Average Value Model (Continuous operation)*

The average value model of the MMI allows for simulating the system without introducing harmonics created by switching events. The circuit parameter values are the same as those listed for the circuit diagram in the previous section and are listed in Table III. The equations for the average value model are provided below and are dependent upon whether the MMI boost converter is operating in a continuous or discontinuous mode of operation. The equations presented below only represent the continuous mode of operation.

The derivative of the current through  $L_1$  is

$$pi_{L1} = \frac{(v_{in} - i_{L1}R_1 - \bar{v}_{dc})}{L_1}, \quad (9)$$

where  $\bar{v}_{dc}$  is the average value of the voltage across  $SW_1$  and is defined as

$$\bar{v}_{dc} = v_{C1}(1 - D), \quad (10)$$

where  $v_{C1}$  is the voltage across  $C_1$  and  $D$  is or duty ratio. The derivative of the voltage across  $C_1$  is

$$pv_{C1} = \frac{(\bar{i}_{dc} - \bar{i}_{ac})}{C_1}, \quad (11)$$

where  $\bar{i}_{dc}$  is the average value of the current out of the boost converter and  $\bar{i}_{ac}$  is the average value of the current into the inverter.  $\bar{i}_{dc}$  is defined as

$$\bar{i}_{dc} = i_{L1}(1 - D) \quad (12)$$

and  $\bar{i}_{ac}$  is defined as

$$\bar{i}_{ac} = \frac{v_{ac}i_{L2}}{v_{C1}}. \quad (13)$$

The derivative of the current through  $L_2$  is

$$pi_{L2} = \frac{(\bar{v}_{ac} - i_{L2}R_2 - v_{C2})}{L_2}, \quad (14)$$

where the total inductance of the filter,  $L_2$ , is defined in (4), the resistance  $R_2$  is defined in (5), and  $\bar{v}_{ac}$  is the average value of the voltage across the output of the inverter defined by

$$\bar{v}_{ac} = mv_{C1} \sin(\varpi_1 t + \theta), \quad (15)$$

where  $m$  is the amplitude modulation ratio,  $\varpi_1$  is the fundamental frequency of the output, and  $\theta$  is the phase angle of the output waveform. The derivative of the voltage across  $C_2$  is

$$pv_{C2} = \frac{(i_{L2} - i_{out}N1N2)}{C_2}, \quad (16)$$

where  $N1N2$  is the turns ratio of  $X_{frm}$ .

The average value model of the MMI was simulated using Matlab [2] and a very crude control design. The results are plotted in Figure 3 through Figure 5. Note that this average value model only represents the continuous mode of operation. Most parasitic effects are not represented in this model except for the resistance of the inductors. All other parasitics and the thermistor  $R_t$  are not represented in the simulation.

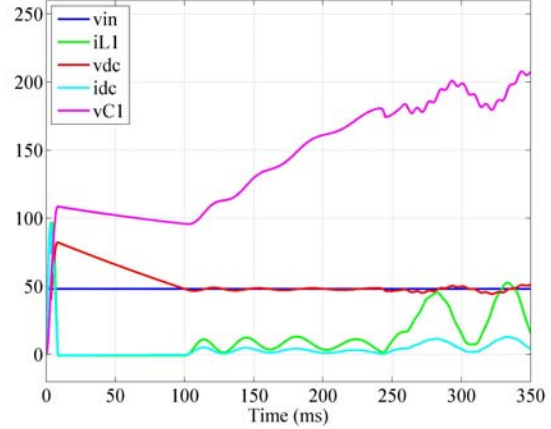


Figure 3. Example simulation results of the average value model. Boost converter waveforms.

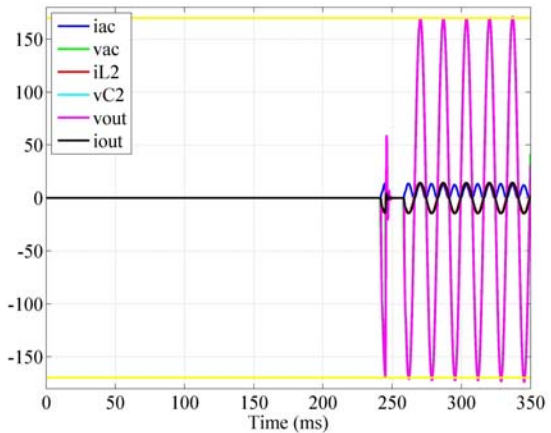


Figure 4. Example simulation results of the average value model. Inverter waveforms

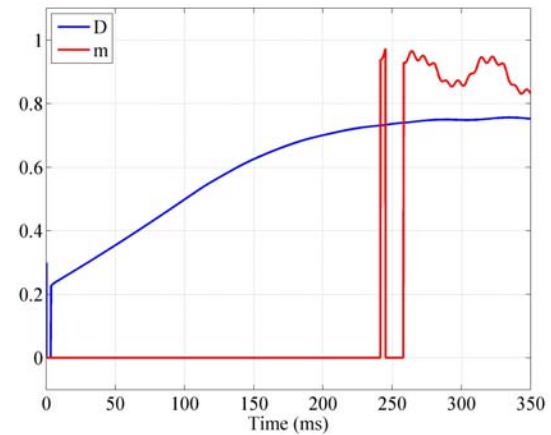


Figure 5. Example simulation results of the average value model. Controller waveforms

## II. DUTY RATIO

In the continuous mode of operation the duty ratio required to achieve a desired capacitor voltage  $v_{C1}$  for a given input voltage is defined as

$$D = 1 - \frac{v_{in}}{v_{C1}}. \quad (17)$$

Duty ratios equal to one are not achievable because of rise and fall times of switching events. To ensure that a valid range of operation is achievable the duty ratio is plotted, Figure 6, over the desired input voltage range for three values of  $v_{C1}$ .

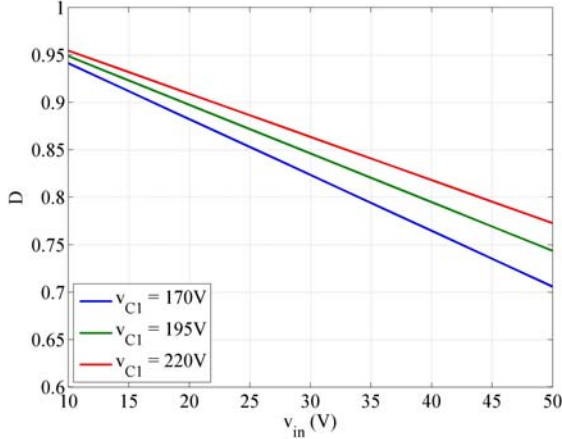


Figure 6. Duty ratio for several  $v_{C1}$  voltages.

## III. CONTINUOUS VERSUS DISCONTINUOUS OPERATION

At the boundary between continuous and discontinuous operation the current  $i_{L1}$  reaches zero just at the time that  $SW_1$  is turned on therefore satisfying the equation

$$\Delta i_{L1} = \frac{(v_{in} - i_{L1}R_1 - V_{SW1on})}{L_1} \Delta t_{on} = i_{L1pk}, \quad (18)$$

where  $\Delta i_{L1}$  is the change in current while  $SW_1$  is on,  $V_{SW1on}$  is the voltage drop across  $SW_1$  in the on state, and  $i_{L1pk}$  is the peak value of  $i_{L1}$  during a switching cycle. Since  $\Delta i_{L1} = i_{L1pk}$  the boundary value current can be defined as

$$i_{L1B} = \frac{1}{2} \Delta i_{L1}. \quad (19)$$

Combining (18) and (19) and solving for  $L_1$  results in

$$L_1 = \left( \frac{v_{in} - V_{SW1on} - R_1}{i_{L1B}} \right) \frac{D}{2f_{sw}}, \quad (20)$$

which allows for an estimate for the required input inductance for a given duty ratio  $D$ , switching frequency  $f_{sw}$ , and boundary current  $i_{L1B}$ . The following three plots of this equation allow the inductance to be chosen

based on input voltage, duty ratio, and input power.  $R_1$ ,  $R_t$ , and  $V_{SW1on}$  are assumed to be zero for this analysis. Power is calculated as

$$P_{in} = \frac{v_{in}}{i_{L1B}}. \quad (21)$$

Figure 7 through Figure 9 use the same switching frequency  $f_{sw}$ , resistance  $R_1$ , and switch voltage  $V_{SW1on}$ . The difference between the three plots is the input voltage  $v_{in}$ . Values of 12V, 30V, and 48V were investigated.

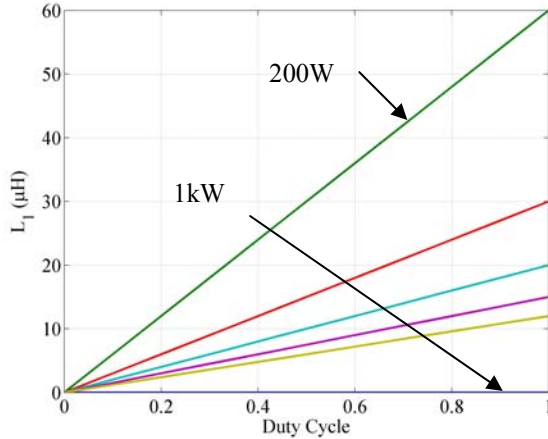


Figure 7. Input inductance vs duty ratio. ( $f_{sw} = 6\text{kHz}$ ,  $v_{in} = 12\text{V}$ ,  $R_1 = 0\Omega$ ,  $V_{SW1on} = 0\text{V}$ )

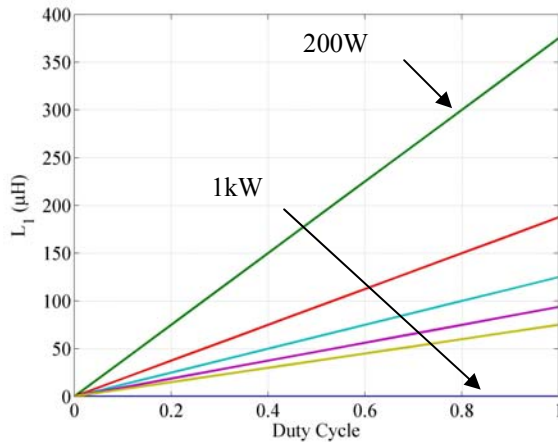


Figure 8. Input inductance vs duty ratio. ( $f_{sw} = 6\text{kHz}$ ,  $v_{in} = 30\text{V}$ ,  $R_1 = 0\Omega$ ,  $V_{SW1on} = 0\text{V}$ )

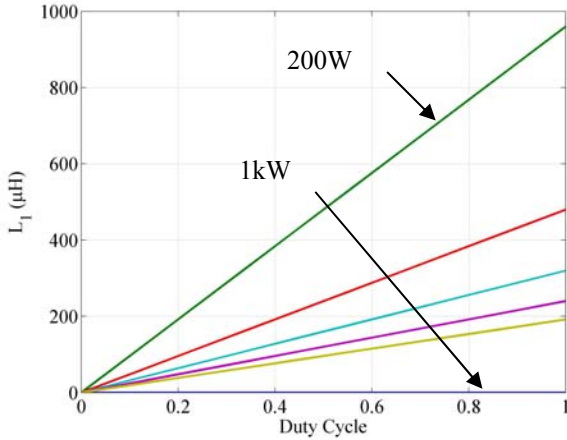


Figure 9. Input inductance vs duty ratio. ( $f_{sw} = 6\text{kHz}$ ,  $v_{in} = 48\text{V}$ ,  $R_l = 0\Omega$ ,  $V_{SW1on} = 0\text{V}$ )

From Figure 7 through Figure 9 it can be seen that higher levels of input voltage require larger input inductances in order to stay in continuous operation. From Figure 9 an inductance value of 1mH will ensure that the boost converter will be in the continuous mode of operation for power levels greater than 200W and an input voltage of 48V.

Solving (20) for  $i_{L1B}$  results in

$$i_{L1B} = \frac{v_{in} - V_{SW1on}}{2f_{sw}L_1 + DR_l} D, \quad (22)$$

which is used to generate Figure 10. In this figure as long as the current is greater than  $i_{L1B}$  for a given  $v_{in}$  and  $D$  the boost converter will be in the continuous mode of operation.

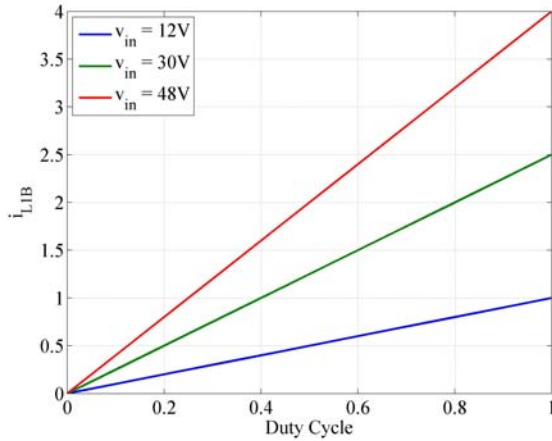


Figure 10. Estimated boundary current between continuous and discontinuous modes of operation. ( $f_{sw} = 6\text{kHz}$ ,  $L_1 = 1.0\text{mH}$ ,  $R_l = 0\Omega$ ,  $V_{SW1on} = 0\text{V}$ )

#### IV. DC LINK VOLTAGE RIPPLE

The capacitance,  $C_1$ , necessary to keep the voltage ripple due to switching of the boost converter at a desired level can be calculated using

$$C_1 = \frac{P_{out}D}{\Delta v_{C1}v_{C1}f_{sw}}, \quad (23)$$

which assumes a constant current out of  $C_1$ . Values of  $C_1$  versus  $D$  are plotted below for a voltage ripple of 1%.

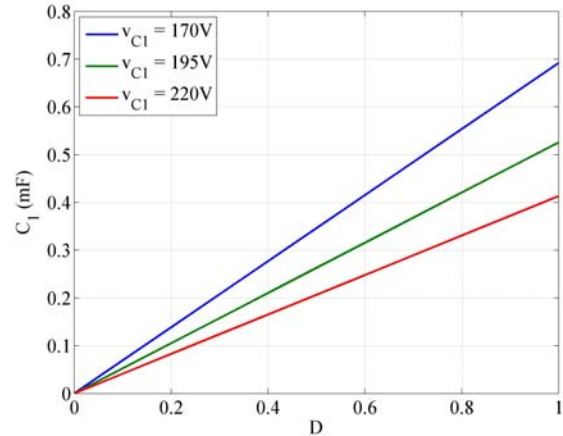


Figure 11. DC link capacitance needed for desired voltage ripple caused by boost converter switching. ( $f_{sw} = 6\text{ kHz}$ ,  $P_{out} = 1.2\text{ kW}$ ,  $\Delta v_{C1} = 1\% \text{ of } v_{C1}$ )

This capacitance value can also be considered in regards to how long the voltage will stay above a given level when the input power is lost. This time period provides some opportunity for the controller to react and bring the output down more gracefully. The voltage droop can be calculated as

$$v_{C1} = \sqrt{\frac{2E_s - 2P_{out}t}{C_1}}, \quad (24)$$

where

$$E_s = \frac{1}{2}C_1v_{C1}^2. \quad (25)$$

From Figure 12 it can be seen that a capacitance of 5 mF will provide about 15ms of operation before an initial voltage of 195 V drops below 170V mark and the inverter enters into a mode of over modulation if  $N1N2$  is 1:1. Below this voltage additional harmonics will be introduced into the output waveform.

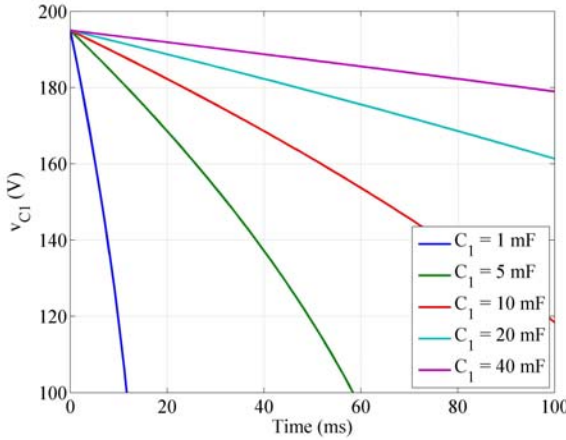


Figure 12. Voltage drop on  $C_1$ . ( $P_{in} = 0$  kW,  $P_{out} = 1.2$  kW)

## V. AMPLITUDE MODULATION RATIO

The amplitude modulation ratio (from this point forward referred to as the modulation ratio)

$$m = \frac{V_{pk}}{v_{C1}}, \quad (26)$$

controls the peak value of the voltage out of the inverter as can be seen in (15). The turns ratio of the transformer must be considered when selecting  $V_{pk}$ . For this power supply the output voltage is required to be 120 Vrms therefore the peak value of the fundamental out of the inverter must be regulated to

$$V_{pk} = \frac{120\sqrt{2}}{N1N2}. \quad (27)$$

From Figure 13 choosing an isolation transformer with a 1:1 turns ratio will keep the modulation ratio below one as long as  $v_{C1}$  is greater than 170 V.

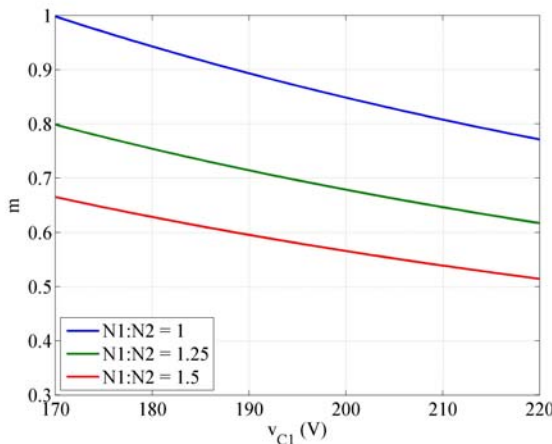


Figure 13. Modulation ratio for a few transformer turn ratios.

## VI. OUTPUT FILTER

The output filter cutoff frequency of 600Hz was chosen to be an order of magnitude less than the 6kHz switching frequency and an order of magnitude greater than the fundamental frequency 60Hz. This analysis neglects  $R_2$  when calculating  $L_2$  versus  $C_2$ .

$$L_2 = \frac{1}{C_2 \omega_c^2}, \quad (28)$$

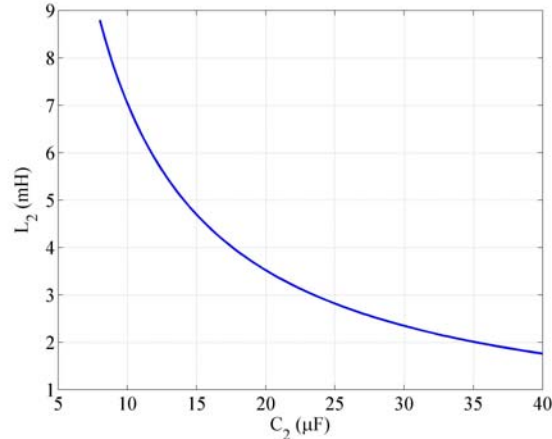


Figure 14. Estimated filter inductor for a given filter capacitor. ( $f_c = 600$ Hz,  $R_2 = 0\Omega$ )

## VII. OUTPUT TRANSFORMER

An output transformer is not required to achieve the required output voltage as can be observed by the modulation ratio calculations plotted in Figure 13. However, an isolation transformer will provide some protection to the power supply and allow the ground connections to be separated.

## VIII. BOOST CONTROL

A place holder for the Boost control was put in the simulation. Stability and robustness over the entire operating range were not analyzed or tested. All signals into the controller are filtered with a double pole low pass filter  $f_c = 600$ Hz.

## IX. INVERTER CONTROL

A place holder for the Inverter control was put in the simulation. Stability and robustness over the entire operating range were not analyzed or tested. All signals are filtered with a single pole low pass filter  $f_c = 600$ Hz.

## X. THERMAL ANALYSIS

This analysis is based on the maximum average current flowing through each device. Power dissipated in a switch is estimated as

$$P_{SW} = \bar{i}_{SW} V_{SWcond} + \frac{1}{2} \bar{i}_{SW} \bar{v}_{SWopen} (t_r + t_f) f_{sw}, \quad (29)$$

where  $\bar{i}_{SW}$  is the average current through the switch,  $V_{SWcond}$  is the conduction voltage drop across the switch,  $\bar{v}_{SWopen}$  is the voltage across the switch while open,  $t_r$  is the rise time of the voltage across the switch when opening,  $t_f$  and is the fall time of the voltage across the switch when closing. A similar equation can be formulated for the diode. Equation (29) along steady state thermal circuit diagrams were used to estimate the junction temperature of each of the semiconductor devices. An analysis at full power for each three different input voltage levels was performed.

#### A. Boost converter with heat sink fan

The circuit diagram is provided in Figure 1 and includes blocks representing the controllers. With the heat sink fan on the boost inverter can run at full power at input voltages as low as 33 V if the ambient temperature is 30 °C. The thermal circuit for the boost converter is provided in Figure 15 and the parameters that were used in the evaluation are provided in Table IV. The heat sink temperature and semiconductor junction temperatures are plotted in Figure 16 and Figure 17. In Figure 17 it can be seen that under these conditions the diode junction temperature reaches 150 °C and the device will be at risk of damage. Therefore the diode is the limiting component.

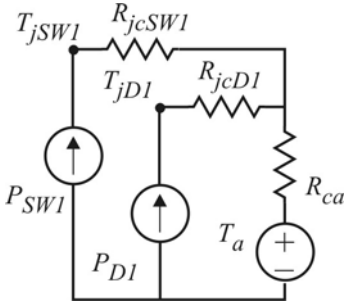


Figure 15. Circuit for thermal analysis.

Table IV. Boost converter thermal analysis parameters.

output power	$P_{out}$	1.2 kW
switching frequency	$f_{sw}$	6 kHz
input voltage	$v_{in}$	33 V <sup>1</sup>
DC link voltage	$v_{C1}^*$	195 V
Heatsink thermal resistance	$R_{ca}$	0.08 °C/W
$SW_1$		
thermal resistance	$R_{jc}$	0.485 °C/W
rise time	$t_r$	80 ns
fall time	$t_f$	250 ns
conduction voltage	$V_{SWcond}$	2.2 V
$D_1$		
thermal resistance	$R_{jc}$	0.955 °C/W
rise time	$t_r$	150 ns
fall time	$t_f$	150 ns
conduction voltage	$V_{SWcond}$	2.6 V

<sup>1</sup> This is the minimum input voltage that this power supply can be operated from at full power and an ambient temperature of 30 °C.

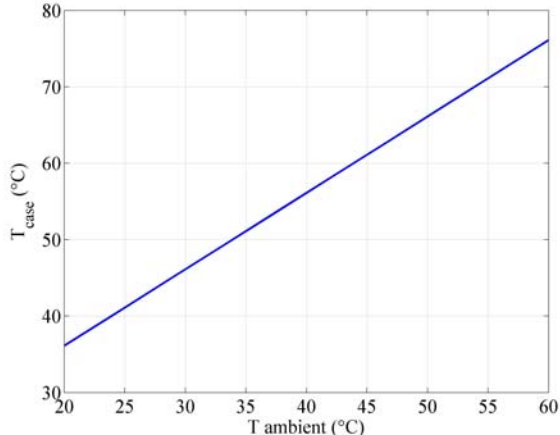


Figure 16. Estimated heat sink temperature.

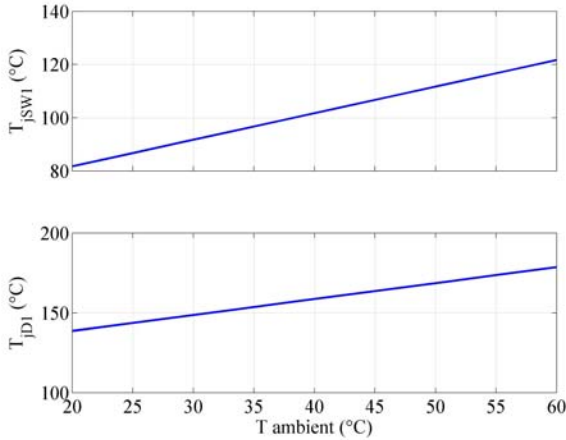


Figure 17. Estimated junction temperatures for  $SW_1$  and  $D_1$ .

### B. Boost converter without heat sink fan

The circuit diagram is provided in Figure 1 and includes blocks representing the controllers. With the heat sink fan on the boost inverter can run at full power at input voltages as low as 46 V if the ambient temperature is 30 °C. The thermal circuit for the boost converter is provided in Figure 15 and the parameters that were used in the evaluation are provided in Table V. The heat sink temperature and semiconductor junction temperatures are plotted in Figure 18 and Figure 19. In Figure 19 it can be seen that under these conditions the diode junction temperature reaches 150 °C and the device will be at risk of damage. Therefore the diode is the limiting component.

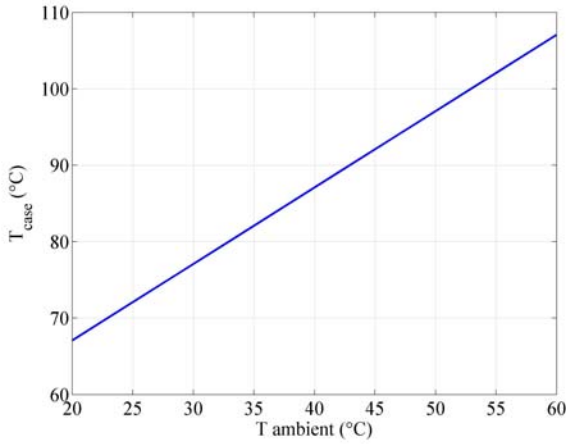


Figure 18. Estimated heat sink temperature.

Table V. Boost converter thermal analysis parameters.

output power	$P_{out}$	1.2 kW
switching frequency	$f_{sw}$	6 kHz
input voltage	$v_{in}$	46 V <sup>1</sup>
DC link voltage	$v_{C1}^*$	195 V
Heat sink thermal resistance (estimated)	$R_{ca}$	0.22 °C/W <sup>2</sup>
$SW_1$		
thermal resistance	$R_{jc}$	0.485 °C/W
rise time	$t_r$	80 ns
fall time	$t_f$	250 ns
conduction voltage	$V_{SWcond}$	2.2 V
$D_1$		
thermal resistance	$R_{jc}$	0.955 °C/W
rise time	$t_r$	150 ns
fall time	$t_f$	150 ns
conduction voltage	$V_{SWcond}$	2.6 V

<sup>1</sup> This is the minimum input voltage that this power supply can be operated from at full power and an ambient temperature of 30 °C.

<sup>2</sup> This thermal resistance is an estimated value based on scaling the size from other natural convection heat sinks.

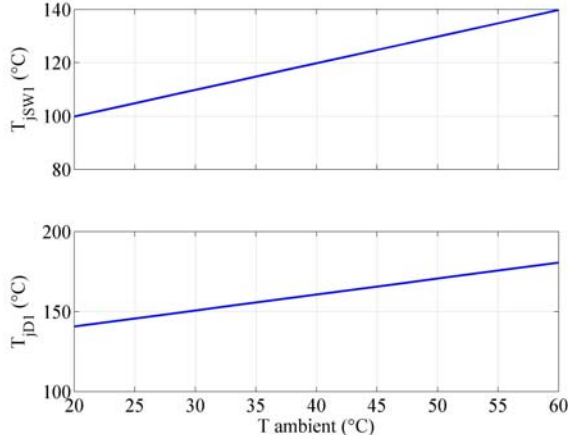


Figure 19. Estimated junction temperatures for  $SW_1$  and  $D_1$ .

### C. Inverter

The thermal performance of the inverter is independent of the MMI input voltage but will be somewhat dependent upon the DC link voltage. The thermal circuit for the H-bridge is provided in Figure 20 and the parameters that were used in the evaluation are provided in Table VI. The heat sink temperature and semiconductor junction

temperatures are plotted in Figure 21, Figure 22 and Figure 23. In Figure 22 and Figure 23 switch junction temperatures do not reach 150 °C even at ambient temperatures as high as 60 °C. Therefore the boost converter will reach thermal limitations prior to the inverter reaching thermal limitations.

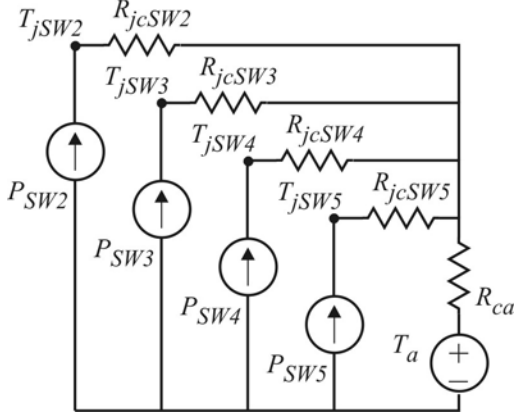


Figure 20. Circuit for thermal analysis.

Table VI. Inverter thermal analysis parameters.

output power	$P_{out}$	1.2 kW
switching frequency	$f_{sw}$	6 kHz
input voltage	$v_{in}$	48 V
DC link voltage	$v_{C1}^*$	195 V
Heat sink thermal resistance (estimated)	$R_{ca}$	0.22 °C/W <sup>1</sup>
$SW_2, SW_3, SW_4, SW_5$		
thermal resistance	$R_{jc}$	0.485 °C/W
rise time	$t_r$	80 ns
fall time	$t_f$	250 ns
conduction voltage	$V_{SWcond}$	2.2 V

<sup>1</sup> This thermal resistance is an estimated value based on scaling the size from other natural convection heat sinks.

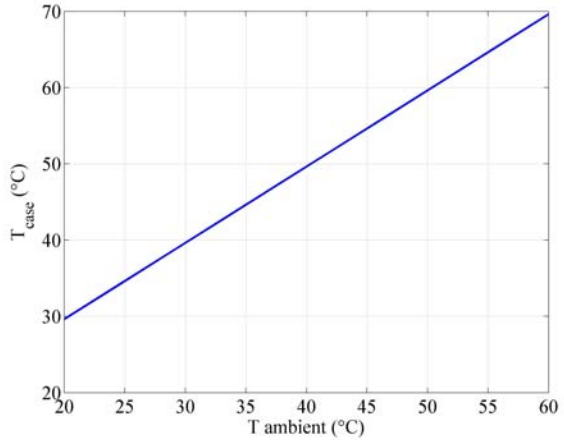


Figure 21. Estimated heat sink temperature for  $SW_2$  through  $SW_5$ .

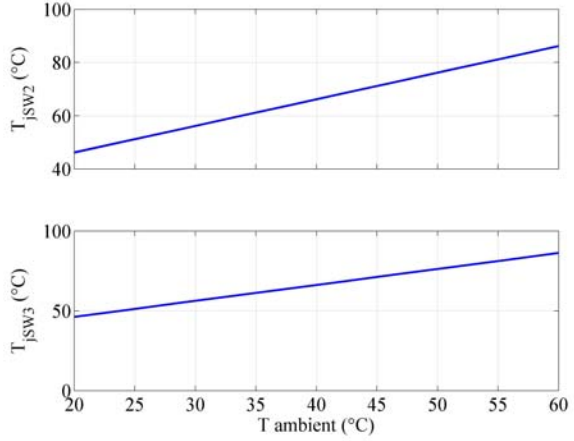


Figure 22. Estimated junction temperatures for  $SW_2$  and  $SW_3$ .

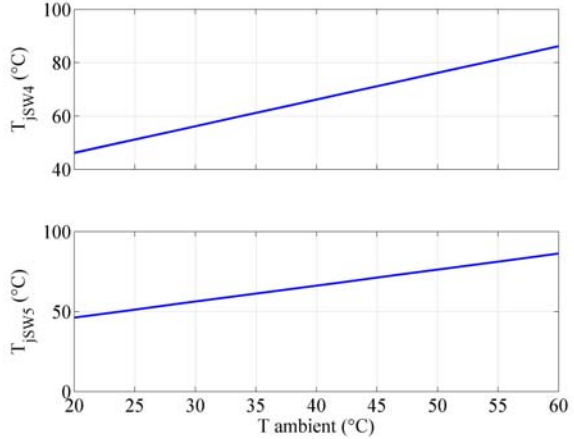


Figure 23. Estimated junction temperatures for  $SW_4$  and  $SW_5$ .

## XI. COMPONENT BASED POWER DERATING

Operational limitations of the MMI need to be limited to the operating range of the components within the MMI. Note that the MMI can operate over a large range of input voltages. However, the input current range is limited to a maximum of 25 Adc by the design of the boost inductor  $L_1$  and 10 Arms by the design of the filter inductors  $L_{2a}$  and  $L_{2b}$ . Since the output of the MMI is regulated to be a 120 Vrms sinusoid the maximum output power is 1.2 kW. However, in order to ensure that  $L_1$  is operating within the designed current limitations the input of the MMI must be derated as the input voltage decreases. Figure 24 contains a plot of the power versus input voltage. Note that for input voltages greater than 48 V the input power is still limited to 1.2 kW but the limiting components become the filter inductors  $L_{2a}$  and  $L_{2b}$  at the MMI output.

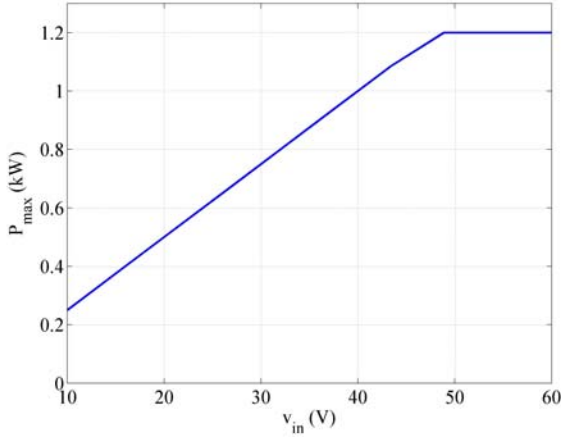


Figure 24. Maximum input power versus input voltage.

## XII. CONDUCTION BASED POWER DERATING

Due to the low input voltage, the saturation voltage  $V_{SWcond}$  across  $SW_1$ , and the resistance  $R_1$  there is a maximum input power for a given input voltage. Note that any resistance or voltage drops external to the MMI (for example internal to the solar panel) will affect this limitation as well but are not being included in these calculations. Based on these parameters the maximum input current is

$$i_{L1max} = \frac{v_{in} - V_{SWcond}}{R_1}, \quad (30)$$

which can be used to estimate the maximum input power

$$P_{max} = v_{in} i_{L1max}. \quad (31)$$

Using these equations  $i_{L1max}$  and  $P_{max}$  are plotted in Figure 25 and Figure 26 with  $V_{SWcond} = 2.8$  V. In Figure 26 it is shown that for an input resistance  $R_1 > 0.1 \Omega$  the desired power of 1 kW is only achievable for input voltages greater than 12 V. For voltages less than this the power supply will need to be derated. Note that the input resistance due to the inductance  $L_1$  is expected to be less than 15 mΩ.

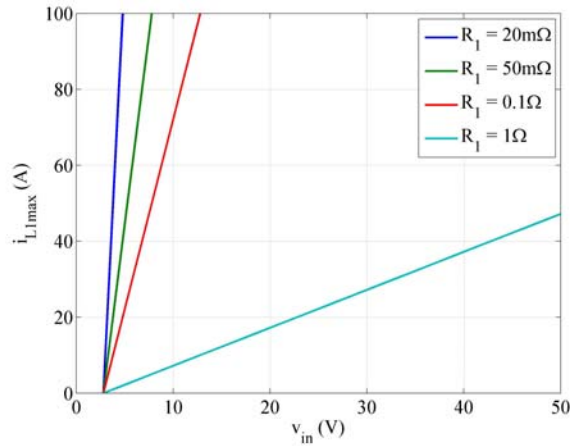


Figure 25. Maximum input current, limited by voltage drops and resistances.

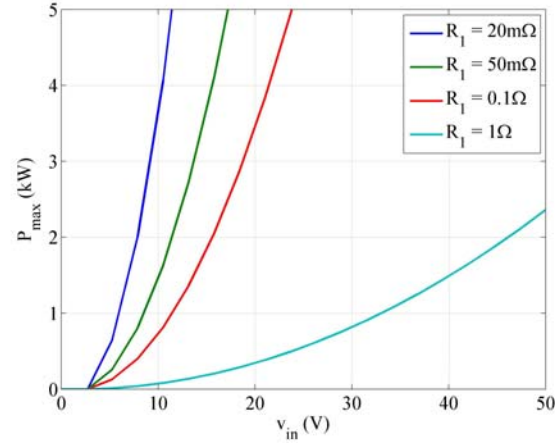


Figure 26. Maximum input power, limited by voltage drops and resistances.

## XIII. SENSOR SIGNAL FILTERS

All sensor signals with bandwidths greater than 600Hz are filtered with a 600 Hz second order low pass Butterworth filter. The circuit diagram and the layout are provided in Figure 27 and Figure 28 below.

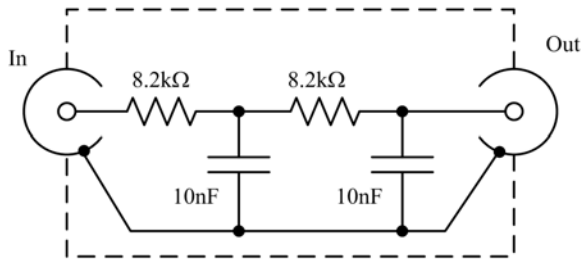


Figure 27. Signal filter.

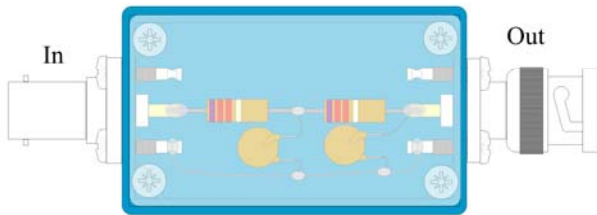


Figure 28. Signal filter layout.

#### XIV. INPUTS AND OUTPUTS

Table VII. Power Connections

1	DC input 0 V – 250 V, 25 A max
2	AC output 0 V rms – 120 Vrms, 10 A max
3	120 V AC power source for controls, 5 A

Table VIII. Sensor and fault signals

1	$v_{in}$	Input Voltage, filtered at 600 Hz, BNC
2	$i_{L1}$	Current through inductor $L_1$ , filtered at 600 Hz, BNC
3	$v_{C1}$	Voltage across $C_1$ , filtered at 600 Hz, BNC
4	$i_{L2}$	Current through inductor $L_2$ , filtered at 600 Hz, BNC
5	$v_{C2}$	Voltage across $C_2$ , filtered at 600 Hz, BNC
6	$v_{out}$	Voltage across the contactor, $Con_1$ , output, filtered at 600 Hz, BNC
7	$i_{out}$	Current out of MMI, filtered at 600 Hz, BNC
8		Boost converter thermal switch, BNC
9		SW1 over current, fiber
10		Bridge fault, fiber
11		Bridge leg A over current, fiber
12		Bridge leg B over current, fiber

Table IX. Control signals

1	$G_{SW1}$	Gate signal for $SW_1$ , fiber
2	$G_{SW2}$	Gate signal for $SW_2$ , fiber
3	$G_{SW3}$	Gate signal for $SW_3$ , fiber
4	$G_{SW4}$	Gate signal for $SW_4$ , fiber
5	$G_{SW5}$	Gate signal for $SW_5$ , fiber
6		Contactor, BNC

#### XV. PHOTOGRAPHS OF THE MMI



Figure 29. MMI enclosure with ruler..



Figure 30. MMI DC input side



Figure 31. MMI AC output side

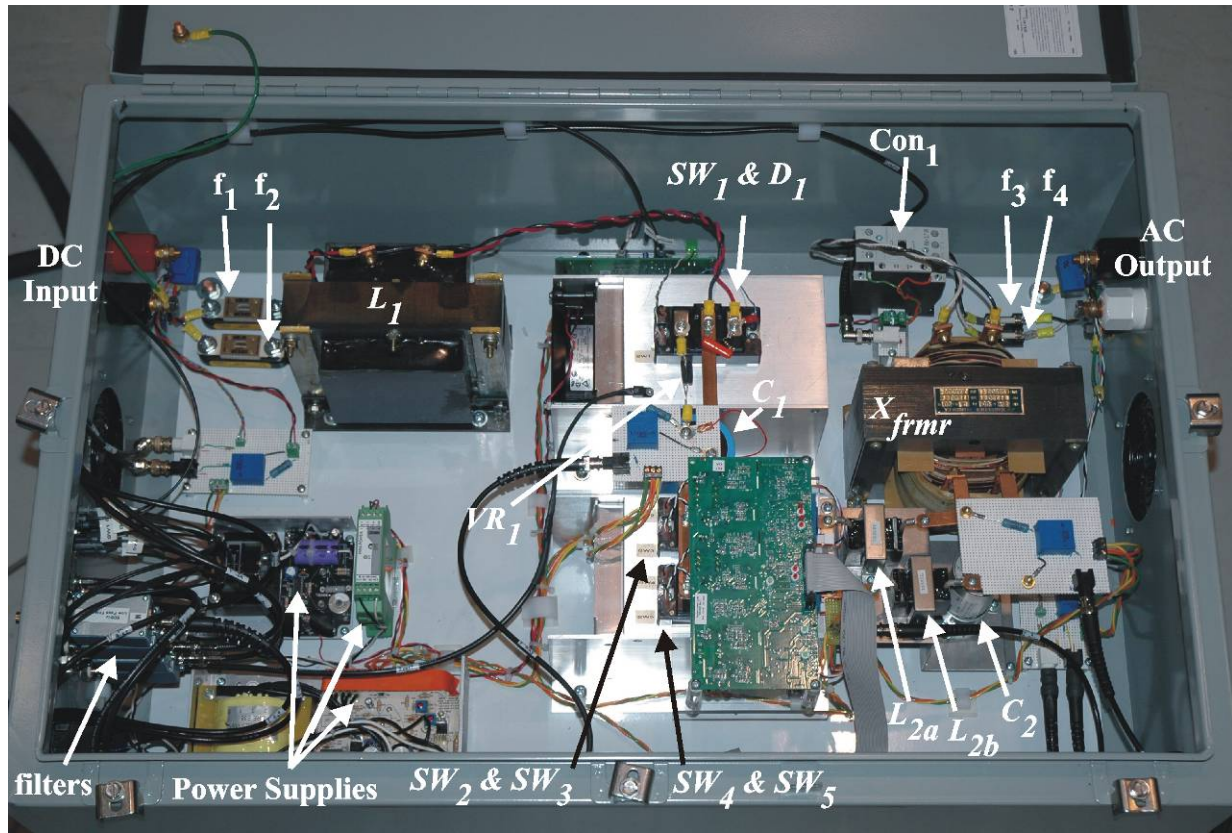


Figure 32. MMI interior



Figure 33. Picture of the signal inputs and outputs

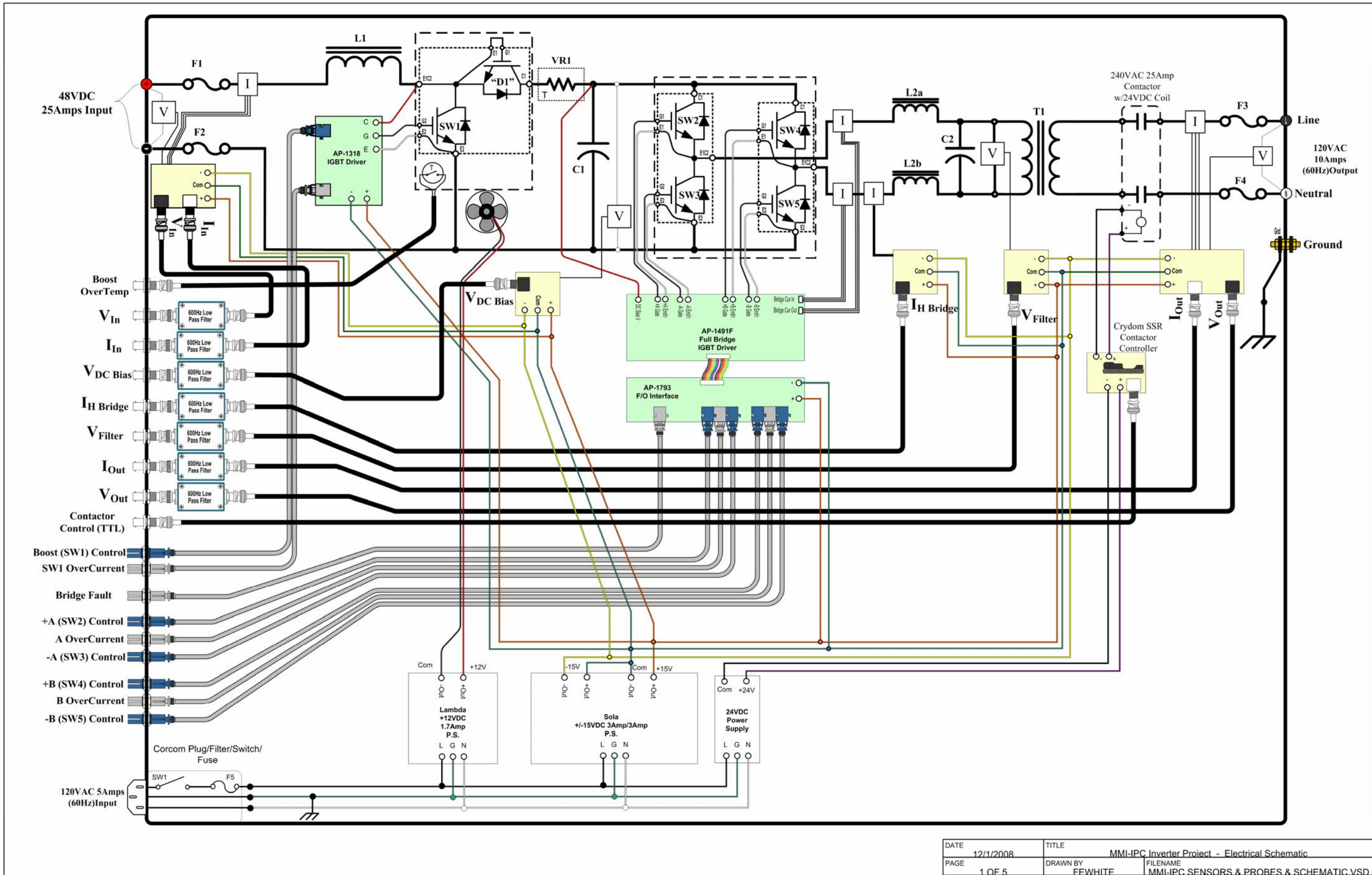
## XVI. REFERENCES

- [1] N. Mohan, T.M. Undeland, W.P. Robbins, "Power Electronics: Converters, Applications, and Design," John Wiley & Sons, Inc., 1995.
- [2] MATLAB The Language of Technical Computing, The MathWorks, Inc., 3 Apple Hill Drive, Natick, MA 01760-2098 USA, [info@mathworks.com](mailto:info@mathworks.com).
- [3] Jim Puissant, Ktech, (505) 845-7383, [jgpuiss@sandia.gov](mailto:jgpuiss@sandia.gov).

## XVII. APPENDIX - PARTS LIST

Item	Symbol	Tech. Specs.	Quantity	Maufac.	Maufac Part#	Vendor	Vendor Part#	Part Quantity	Unit Cost	Extended Cost	Date Ordered	Ordered by:	Type Order/(PO# if applies)	Quan.	Date Rec'd	Delivery Time (days)	Quan.	Date Rec'd	Delivery Time (days)
1	L1	1.0 mH, 25A, 250V, 10kHz	3	L/C Magnetics	5275L14d (9" x 9" x 9")	L/C Magnetics	5275L14d	3	\$1,552.00	\$4,656.00	7/28/2008	Christina	P-Card						
2	L2a,L2b	1.0 mH, 25A, 250V, 10kHz	6	L/C Magnetics	5275L1Bb (4" x 4" x 4")	L/C Magnetics	5275L1Bb	6	\$795.00	\$4,770.00	7/28/2008	Christina	P-Card						
3	C1	5.2 mF, 250V, 0.2ESR	3	Cornell-Dubilier	CGS4221250W5L (4.2mF, 250VDC)	Newark	69K1868	3	\$60.40	\$181.20	7/31/2008	Christina	P-Card	3	8/4/2008	4			
4	C2	36 uF, 250V, 0.2ESR	3	Cornell-Dubilier	SFC37535K291B (35uF, 370VDC)	Newark	66K4139	3	\$37.17	\$111.51	7/31/2008	Christina	P-Card	3	8/4/2008	4			
5	D1	Fast Recovery Power Diode, 250A, 250V, 10kHz, Rth j-c = XX °C/W, Rth c-a = XX °C/W	0					0		\$0.00									
6	SW1	Fast Recovery Dual IGBT, 25A, 250V, 10kHz, Rth j-c = XX °C/W, Rth c-a = XX °C/W	3	Powerex	CM75DU-12F (Dual 75A,600V)	Richardson Electronics	CM75DU-12F	3	\$50.57	\$151.71	7/31/2008	Christina	P-Card						
7	SW2,SW3	Fast Recovery Dual IGBT, 25A, 250V, 10kHz, Rth j-c = XX °C/W, Rth c-a = XX °C/W	3	Powerex	CM75DU-12F (Dual 75A,600V)	Richardson Electronics	CM75DU-12F	3	\$50.57	\$151.71	7/31/2008	Christina	P-Card						
8	SW4,SW5	Fast Recovery Dual IGBT, 25A, 250V, 10kHz, Rth j-c = XX °C/W, Rth c-a = XX °C/W	3	Powerex	CM75DU-12F (Dual 75A,600V)	Richardson Electronics	CM75DU-12F	3	\$50.57	\$151.71	7/31/2008	Christina	P-Card						
9	Xfrm	Isolation transformer, 1.2kVA, 60Hz, NI:1=1:1, 300V isolation	3	L/C Magnetics	5275L3c (7.5" x 7.5" x 7.5")	L/C Magnetics	5275L3c	3	\$575.00	\$1,725.00	7/28/2008	Christina	P-Card						
10	Enclosure		3	Hammond	Steel 1418N412 (36" x 24" x 12")	Allied Electronics	8061061	3	\$576.19	\$1,728.57	7/31/2008	Amy	P-Card	1	8/1/2008	1	2	8/8/2008	8
11	Fans	4.72" x1.54", 12VDC/0.5A, 110CFM	0	COMAIR-ROTRON	MD12R2.028868	Allied Electronics	599-0288	3	\$49.58	\$148.74	7/31/2008	Amy	P-Card	3	8/4/2008	4			
12	Vent Screens	4.72" "Finger Guards"	12	COMAIR-ROTRON	550481 (4.72" -Zinc plated steel wire)	Allied Electronics	599-5504	12	\$1.16	\$13.92	7/31/2008	Amy	P-Card						
13	Heat sink #1		3	Aavid Thermalloy	476200U00000	Electronics Precepts	476200U00000	3	\$132.90	\$398.70	7/29/2008	Christina	P-Card	3	8/4/2008	6			
14	Heat sink #2		3	Aavid Thermalloy	476200U00000	Electronics Precepts	476200U00000	3	\$132.90	\$398.70	7/29/2008	Christina	P-Card	3	8/4/2008	6			
15	V <sub>C1</sub> sensor	0-250V, 0-600Hz	3	Sandia	Vc1	Sandia	Vc1												
16				Sypris-F.W. Bell	CLSM-10MA	Allied Electronics	595-0004	3	\$30.16	\$90.48	7/31/2008	Amy	P-Card						
17	Rv2	30kΩ, 5W,1% wirewound Resister	3	Ohmite	45F30KE	Allied Electronics	296-5556	12	\$2.56	\$30.72	7/31/2008	Amy	P-Card	12	8/4/2008	4			
18	Rm2	400kΩ, 1/2W, 1% metal film	3	Phoenix Passive Components	MRS25 402R 1%	Newark	97K5808	100	\$0.04	\$3.50	7/31/2008	Christina	P-Card	100	8/6/2008	6			
19																			
20																			
21	i <sub>1,2</sub> Sensor	±10A, 0-600Hz	3	Sypris-F.W. Bell	CLS-25	Allied Electronics	595-0029	3	\$24.27	\$72.81	7/31/2008	Amy	P-Card	3	8/4/2008	4			
22	Rm3	400Ω, 1/2W, 1% metal film	3	Phoenix Passive Components	MRS25 402R 1%	Newark	97K5808	see item 18											
23	V <sub>C2</sub> Sensor	±190V, 0-600Hz	3	Sandia	Vc2	Sandia	Vc2												
24				Sypris-F.W. Bell	CLSM-10MA	Allied Electronics	595-0005	3	\$30.16	\$90.48	7/31/2008	Amy	P-Card						
25	Rv6	15kΩ, 5W,1% wirewound Resister	3	Ohmite	45F15KE	Allied Electronics	296-5527	12	\$2.09	\$25.08	7/31/2008	Amy	P-Card	12	8/4/2008	4			
26	Rm6	316Ω, 1/2W, 1% metal film	3	Phoenix Passive Components	MRS25 316R 1%	Newark	97K5739	100	\$0.04	\$3.50	7/31/2008	Christina	P-Card	100	8/6/2008	6			
27		360Ω, 1/2W, 1% metal film	3	Phoenix Passive Components	MRS253560R 1%	Newark	78K5739	100	\$0.04	\$3.50	7/31/2008	Christina	P-Card						
28																			
29	thermal sensor		3	Honeywell	573T110A120	Border States	573T110A120	6	\$35.00	\$210.00									
30	SW1 Gate driver		3	Applied Power Systems Inc.	AP-1318	Applied Power Systems Inc.	AP-1318	3	\$256.00	\$768.00	7/30/2008	Amy	P-Card						
31	Analog connection		3	Sandia	"IPC Control Interface Assy with signal filtering"			0		\$0.00									
32	Internal power supply	"/+ 15VDC (3Amps),"	3	Sola/Heavy Duty	SLD15-3030-15T	Newark	93K6593	3	\$121.89	\$365.67	7/31/2008	Christina	P-Card	3	8/4/2008	4			
33	Internal power supply	Fan Power Supply - +12VDC (1.7Amps)	3	Sola/Heavy Duty	HSB-12-1.7	Newark	14M5851	3	\$41.51	\$124.53	7/31/2008	Christina	P-Card	3	8/4/2008	4			
34	SW2,3,4,5 Gate Driver		3	Applied Power Systems Inc.	AP-1491F, Full Bridge IGBT Driver	Applied Power Systems Inc.	AP-1491F	3	\$389.00	\$1,167.00	7/30/2008	Amy	P-Card						
35	E/O Interface For Above		3	Applied Power Systems Inc.	AP-1793, IGBT Driver Interface	Applied Power Systems Inc.	AP-1793	3	\$305.00	\$915.00	7/30/2008	Amy	P-Card						
36	Fuse		6	Cooper-Bussman	ANL-35 to ANL-40	Newark	02B2084 or 02B2086	6	\$35.00	\$210.00	7/31/2008	Christina	P-Card	5	8/7/2008	7	1	8/8/2008	8
37	Fuse Holder		6	Cooper-Bussman	Fuseblock 4164	Newark	94F2259	6	\$35.00	\$210.00	7/31/2008	Christina	P-Card	6	8/4/2008	4			
38		Negative temperature coefficient thermistor 2 Ohm	3	AMETHERM	SL22 2R018	Newark	72J6826	12	\$1.80	\$21.60	7/31/2008	Christina	P-Card	12	8/4/2008	4			
39	FO	Capacitor Mounting bracket 2.5in.-2.56in.dia.	3	CDE	VR10A	Newark	60D2292	3	\$2.62	\$7.86	8/5/2008	Christina	P-Card	3	8/8/2008	2			
40	FO	Capacitor Mounting bracket 1.75in.-1.81in.dia.	3	CDE	VR6A	Newark	14F412	3	\$2.59	\$7.77	8/5/2008	Christina	P-Card	3	8/8/2008	2			
41	FO	Fiber Optic Cable Simplex POF 10 meters	2	Avago	HFB-R-RNS010Z	Newark	71K0250	2	\$14.74	\$29.48	8/5/2008	Christina	P-Card	2	8/8/2008	2			
42	FO	Fiber Optic Cable Duplex F 10 meters	2	Avago	HFB-R-RMD010Z	Newark	71K0247	2	\$29.47	\$58.94	8/5/2008	Christina	P-Card						
43	FO	Fiber Optic Connector, Gray	50	Avago	HFB-4501Z	Newark	74K5180	50	\$0.56	\$28.20	8/5/2008	Christina	P-Card	50	8/8/2008	2			
44	FO	Fiber Optic Connector, Blue	50	Avago	HFB-4511Z	Newark	74K5184	50	\$0.56	\$27.78	8/5/2008	Christina	P-Card	50	8/8/2008	2			

## XVIII. APPENDIX – WIRING DIAGRAM



## XIX. APPENDIX – H-BRIDGE CURRENT SENSOR

